PREDICTIONS OF DIOXINS FORMATION IN THE SINTER PLANT FACILITIES.

Aneliza Porto Gonçalves, aneliza@metal.eeimvr.uff.br
Jose Adilson de Castro, adilson@metal.eeimvr.uff.br
Metallurgical and Materials Science Engineering -EEIMVR-UFF, Av. dos Trabalhadores 420 – Vila Sta. Cecília – 27255-125 – Volta Redonda – RJ

Abstract: The iron ore sintering is a complex process involving various physical and chemical phenomena. The raw materials used can vary to a wide extent, from iron ore to dust recycling and several impurities are input and react at high temperature. The process takes place in a moving strand where a mixture of iron ore (sinter feed), fine coke, limestone and water is continuously charged to form a thick bed of approximately 40cm. Along the first meters of the strand the charge is ignited by burners. The hot gas, generated by the combustion of natural gas with air, is then sucked in through the packed bed from the wind boxes placed below the grate. The most concerning toxic substances generated in such conditions are the so-called dioxins and furans consisting of aromatic substances combined with chlorine, hydrogen and oxygen. Models to predict the operational parameters and determine optimum conditions for minimizing the formation and emissions of these substances are of great importance due to the low cost and the ability to investigate conditions which can not be assessed by experimental techniques. In this paper a mathematical model based on the multiphase multi-component transport equations is used to investigate the industrial scale operation and predict the rate formation of these substances. The transport equations are discretized based on the finite volume method and rate equations for transfer of momentum, energy and chemical reactions are used to consider the inter-phase interactions. The model predictions are in agreement with the averaged values measured at the gas outlet of the sinter strand which validated the modeling approach. Measurements of dioxins and furans previously published are confronted with model predictions and selective re-circulating gas technique is proposed as efficient way of drastically reduce the emissions.

Keywords: *dioxins, modeling, computational simulation, sinter strand*

1. INTRODUCTION

The sintering process is a well established process used to furnish raw materials for the blast furnace of the integrated route of steel production. The process is complex and involves various physical and chemical phenomena such as heat, mass and momentum transfer. These phenomena take place simultaneously increasing considerably the complexity of process analysis and control. The raw materials used can vary to a wide extent, from iron ore to dust recycling. The process takes place in a moving strand where a mixture of iron ore (sinter feed), fine coke, limestone and water is continuously charged to form a thick bed of approximately 40-80 cm. Along the first meters of the strand the charge is ignited by burners and the fuel combustion propagate the sinter front. The hot gas, generated by the combustion of natural gas with air, is then sucked in through the packed bed from the wind boxes placed below the grate.

The combustion of fines coke begins at the top of the layers, and as it moves, a relative narrow band of ignition zone moves down through the bed. Several chemical reactions and phase transformations take place within the bed, the materials partially melt when the local temperature reaches the melting temperature and as it moves, the solidification process occurs. The partial melting and diffusion within the materials promotes the particle agglomeration forming a continuous porous sinter cake. In general, the hot gas produced during sintering can also be re-circulated for better thermal efficiency and environmental savings. A schematic view of the sinter machine with recycling gas concept is presented in Fig. 1.

The physicochemical and thermal phenomena involved are complex and numerous. Special mention is made to the phenomena of gas flow through the porous bed, gas-solid heat transfer, drying and several chemical reactions and phase transformations. Several attempts have been made aiming to predict the final properties of the sinter product. One of the most important parameter is the size distribution which influences strongly the sinter performance within the blast furnace. Waters at al (Waters at al, 1989), developed a mathematical model to predict the final size distribution of the sinter, however, as they pointed out, the model did not considered the kinetics of the sintering phenomena, which strongly affect the final size distribution. Kasai et al (Kasai et al, 1991), investigated the influence of the sinter structure into the macroscopic sinter properties.

A detailed explanation of the sintering mechanism and particles interaction were analyzed to clarify the bonding forces. They concluded that the void fraction and specific surface area are the main parameters influencing the cake strength. They also concluded that the significant driving forces of structural changes in the sinter cake are compressive and capillary ones. Akiyama et al(Akiyama et al,1992) investigated the heat transfer properties under the sinter bed conditions and established empirical correlations for the material conductivity. However, there are few comprehensive mathematical models describing the sintering process in an industrial machine such as the usual Dwight-Lloyd. Mitterlehner et al (Mitterlehner et al, 2004), presented a 1-D mathematical model of the sinter strand focusing on the progression speed of the sintering front. Nath et al, (Cumming, et al, 1990, Nath et al, 1997), developed a 2-D mathematical model based on transport equations, however, their analysis considered a few chemical reactions and the rate of phase transformations were simplified.

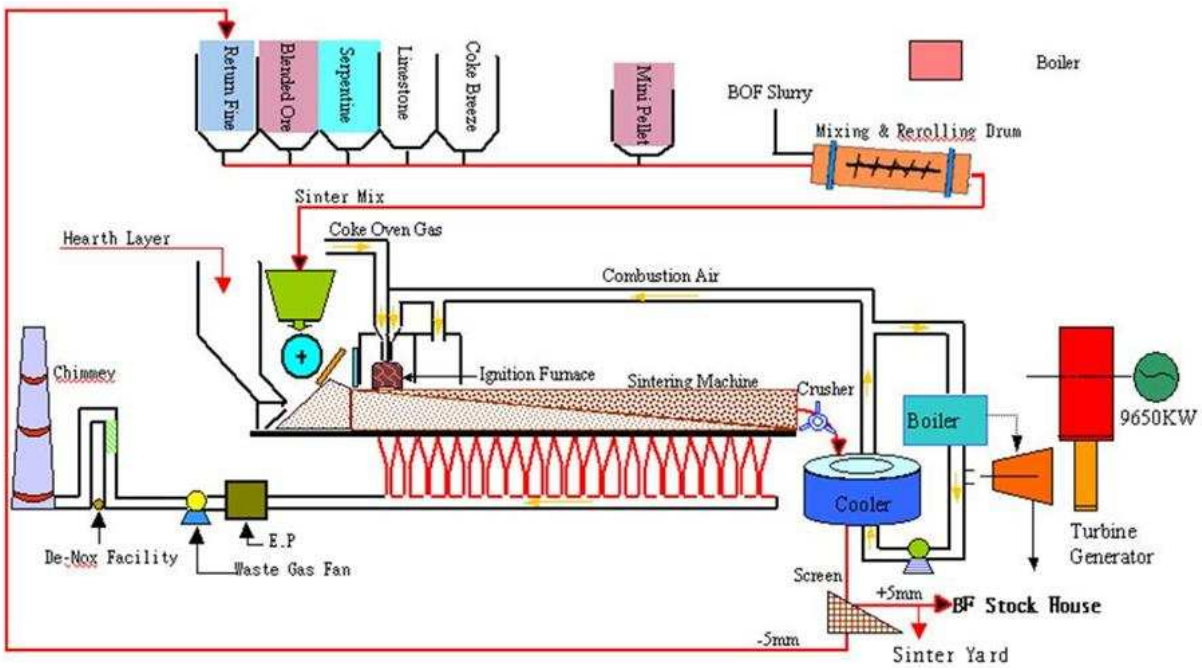

Figure 1 A schematic view of the iron ore sinter facilities and material flow chart.

A more detailed multi-phase model has been developed by Castro et al (Castro et al, 2005) which has been continuously updated (Castro et al, 2006). Therefore, a comprehensive mathematical model able to describe the chemical reactions coupled with momentum, energy and species transport has yet to be continuously improved and applied to simulate the industrial scale of the sintering machine. Moreover, the massive industrial processes using fuels are claimed to reduce all kinds of emissions. One of the most pollutant substances generated within combustion processes carried out at high temperature is the so-called dioxins and furans, toxic substances composed for carbon, hydrogen and chlorine, deriving of combustion processes of organic substance in chlorine presence. In terms of generation of these substances in the steelworks the sintering machine represents higher than 50% of total generation. When compared with other pollution sources, the steelworks represents about 11%, as observed in Fig. 2.

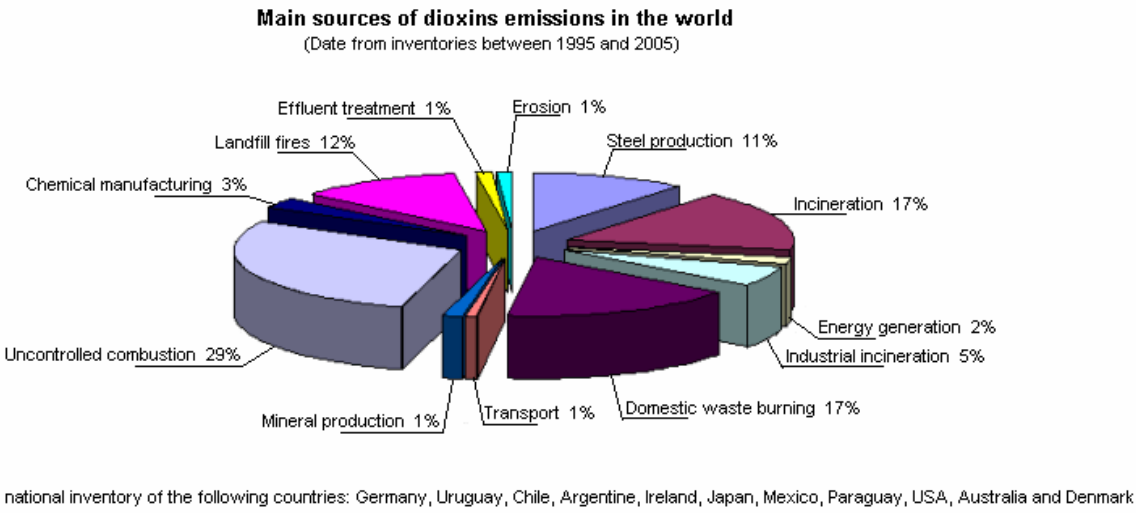

Figure 2 Main sources of dioxin emissions in the world between 1995 and 2005.

To successfully address technologies able to reduce dioxins and furans emissions precise models able to predict and indicate optimum operational conditions has to be developed. In the present work, a 3-dimensional mathematical model of the sinter strand is developed based on the multiphase multi-component concept and detailed interactions between the gas and solid phases are addressed. Within the model framework are considered the following phenomena: a) dynamic interaction of the gas mixture with the solids; b) overall heat transfer of all phases; c) vaporization and condensation of water; d) decomposition of carbonates; e) reduction and oxidation of the iron bearing materials; f) fuel combustion and gasification; g) shrinkage of the packed bed; h) partial melt-solidification of the solids and i) phase changes. This model differs significantly of the former ones due to the concept of multiple and coupled phenomena treatment, three-dimensional treatment of the sinter strand and detailed mechanism of chemical reactions involved in the process.

Therefore, this formulation represent a step forward on the task of constructing a comprehensive mathematical model of the iron ore sinter process capable of considering detailed phenomena which take place in the industrial operation. In this paper the actual sinter process is simulated and compared with industrial data. Afterwards the influence of the fuel quality is investigated and other alternative fuels such anthracite and biomasses are tested in order to indicate rational use of natural resources and develop cleaner industrial processes. Aiming to develop environmentally cleaner processes the dioxin and furans formation is investigated and optimum operation conditions are suggested in order to minimize their emissions.

2. MODELING

The phenomena that occur into the sintering bed mostly define the quality of sinter products. In order to model the process the concept of multiphase and multi-component is assumed. The multiphase principle assumes that momentum, energy and chemical species are exchanged among the phases and the rates of transfer are modeled by semi-empirical correlations. In this work, a two phase system is modeled where the solid phase is regarded as a mixture of solid particles having their own properties. In this framework, the solid phase is behaves like a non-uniform porous media and the mixture rules are applied to account for the individual contribution of each solid component through its volume fraction. The gas occupies the solid phase porosities leading to Eq. (1).

$$\varepsilon_s + \varepsilon_g = 1 \tag{1}$$

$$\varepsilon_s = \sum_{m=1}^{m=ncomponents} f_m \tag{2}$$

Figure 3 illustrates the model concept, phase iteration parameters and boundary conditions for modeling the sinter strand of a commercial scale of iron ore sinter plant. As can be seen, the gas phase is sucked through the sinter bed promoting momentum transfer leading to a strong pressure drop and simultaneously exchanging energy by convective, radiative and chemical reaction processes.

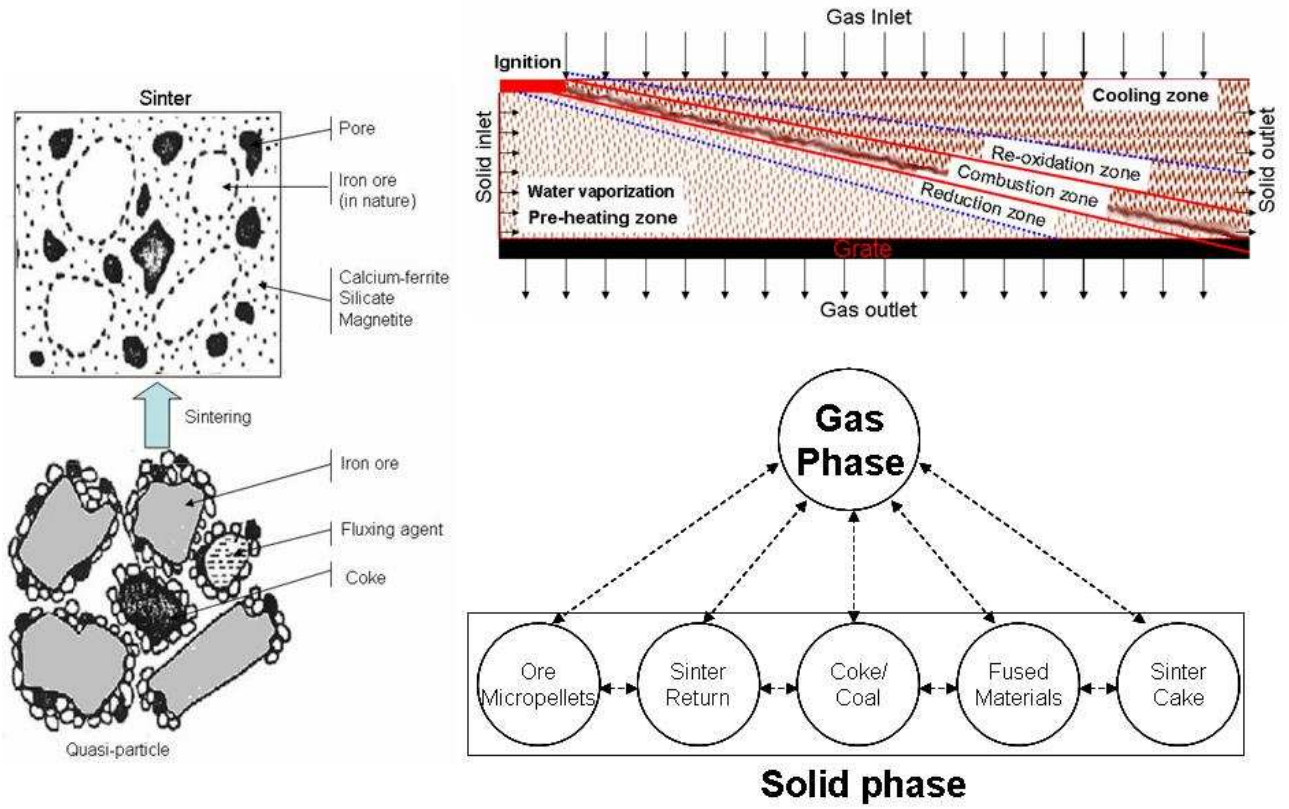

Figure 3 Sintering mechanism, model concept of phase interactions, calculation domain and boundary conditions

2.1 Transport equations

Momentum balance for gas and solid are modeled using Eqs. (3) through (10), respectively.

Gas phase:

Momentum equations:

$$\frac{\partial(\rho_g \varepsilon_g u_j)}{\partial t} + div\,(\rho_g \varepsilon_g \vec{U}_g\, u_j) = div\,[\varepsilon_g\, \mu_g\, grad\,(u_j)] - grad\,(P_g) + F_s^g \tag{3}$$

$$\frac{\partial(\rho_g \varepsilon_g)}{\partial t} + \mathrm{div}(\rho_g \varepsilon_g \vec{U}_g) = \sum_{i=1}^{nreacts} R_i^g \tag{4}$$

Energy equation:

$$\frac{\partial(\rho_g \varepsilon_g h_g)}{\partial t} + \mathrm{div}\,(\rho_g \varepsilon_g \vec{U}_g\, h_g) = \mathrm{div}\left[\varepsilon_g \frac{k_g}{C_{p,g}} \mathrm{grad}\,(h_g)\right] + E_s^g + \sum_{i=1}^{nreacts} R_i^g \Delta h_i \tag{5}$$

Chemical species equations:

$$\frac{\partial(\varepsilon_g \rho_g \phi_{g,k})}{\partial t} + \mathrm{div}\,(\varepsilon_g \rho_g \vec{U}_g \phi_{g,k}) = \mathrm{div}\left[\varepsilon_g \frac{D_k^g}{\varepsilon_g \rho_g} \mathrm{grad}\,(\phi_{g,k})\right] + \sum_{i=1}^{nreacts} R_i^g \beta_k \tag{6}$$

Where the indexes i and k indicate chemical reactions and chemical species, respectively. $\vec{U}$ is velocity field and u_j is velocity component on the directions (j=1,2,3). The subscripts g and s denote the gas and solid phases, respectively.

The solid phase can be expressed in a similar fashion as fallows:

Momentum:

$$\frac{\partial(\rho_s \varepsilon_s u_j)}{\partial t} + \mathrm{div}(\rho_s \varepsilon_s \vec{U}_s\, u_j) = \mathrm{div}[\varepsilon_s\, \mu_s \mathrm{grad}\,(u_j)] - \mathrm{grad}\,(P_s) - F_s^g - F_s^s \tag{7}$$

$$\frac{\partial(\rho_s \varepsilon_s)}{\partial t} + \mathrm{div}\,(\rho_s \varepsilon_s \vec{U}_s) = \sum_{i=1}^{nreacts} R_i^s \tag{8}$$

Energy equation:

$$\frac{\partial(\rho_s \varepsilon_s h_s)}{\partial t} + \mathrm{div}\,(\rho_s \varepsilon_s \vec{U}_s\, h_s) = \mathrm{div}\left[\varepsilon_s \frac{k_s}{C_{p,s}} \mathrm{grad}\,(h_s)\right] - E_s^g + \sum_{i=1}^{nreacts} R_i^s \Delta h_i \tag{9}$$

Chemical species equations:

$$\frac{\partial(\varepsilon_s \rho_s \phi_{s,k})}{\partial t} + \mathrm{div}\,(\varepsilon_s \rho_s \vec{U}_s \phi_{s,k}) = \mathrm{div}\left[\varepsilon_s \frac{D_k^s}{\varepsilon_s \rho_s} \mathrm{grad}\,(\phi_{s,k})\right] + \sum_{i=1}^{nreacts} R_i^s \beta_k \tag{10}$$

The phases and chemical species considered in this model are summarized in table 1. (Austin et al, 1997, Castro et al, 2001,2002, 2005, 2006)

2.2 Boundary and initial conditions

The boundary conditions applied to the set of differential conservation equations of the model are of the inlet and outlet type for the gas phase at the top and the bottom faces, respectively. The energy equation uses as inlet boundary condition the average inflow temperature and at the outlet is assumed no temperature gradient. The inlet composition of the solid phase is specified together with solid temperature. For the velocity field, the gas is suctioned and the pressure

gradient is used to specify the inlet flow rate at the top surface. The other boundaries are of symmetry type, where no flux is assumed, except for the temperature where a heat transfer coefficient is specified.

Table 1 Momentum, energy and chemical species considered to model the sintering process

Equations of the gas phase			
Gas	Momentum	$u_{1,g}$, $u_{2,g}$, $u_{3,g}$, P_g, ε_g	
	Energy	h_g	
	Chemical Species	N_2, O_2, CO, CO_2, H_2O, H_2, SiO, SO_2, CH_4, C_2H_6, C_3H_8, C_4H_{10}, dioxin, furan, chrorobenzene	
Equations of the solid phase			
Solid	Momentum	$u_{1,s}$, $u_{2,s}$, $u_{3,s}$, P_s, ε_s	
	Energy	h_s	
	Chemical Species	Coke breeze	C, Volatiles, H_2O, Al_2O_3, SiO_2, MnO, MgO, CaO, FeS, P_2O_5, K_2O, Na_2O, S_2
		Iron ore	Fe_2O_3, Fe_3O_4, FeO, Fe, H_2O, Al_2O_3, SiO_2, MnO, MgO, CaO, FeS, P_2O_5, K_2O, Na_2O
		Return Sinter (bed)	Fe_2O_3, Fe_3O_4, FeO, Fe, H_2O, Al_2O_3, SiO_2, MnO, MgO, CaO, FeS, P_2O_5, K_2O, Na_2O
		Fused Materials	Fe_2O_3, Fe_3O_4, FeO, Fe, H_2O, Al_2O_3, SiO_2, MnO, MgO, CaO, FeS, P_2O_5, K_2O, Na_2O, $CaO.Fe_3O_4$, $Al_2O_3.MgO$
		Fluxing agent	CaO, H_2O, Al_2O_3, SiO_2, MnO, MgO, TiO_2
		Sinter cake	Fe_2O_3, Fe_3O_4, FeO, Fe, H_2O, Al_2O_3, SiO_2, MnO, MgO, CaO, FeS, P_2O_5, K_2O, Na_2O, $CaO.Fe_3O_4$, $Al_2O_3.MgO$, dioxin, furan

Total of 116 partial differential equations numerically solved using the finite volume technique.

2.3 Source Terms

The interactions between the solid and gas phase is represented though the source terms of each equation. The source terms are due to external forces, interfaces interactions, chemical reactions and phase transformations. This section describes the models used for each of these phenomena.

2.3.1 Momentum sources

$$F_m = 150\mu_g \frac{1}{\left|\vec{U_g} - \vec{U_s}\right|}\left(\frac{\varepsilon_m}{(1-\varepsilon_m)\, d_m \varphi_m}\right)^2 + 1.75\rho_g\left(\frac{\varepsilon_m}{(1-\varepsilon_m)\, d_m \varphi_m}\right) \tag{11}$$

$$F_g^s = -F_s^g = \left[\sum_m f_m F_m\right]\left|\vec{U}_g - \vec{U}_s\right|\left(\vec{U}_g - \vec{U}_s\right) \tag{12}$$

Where ***m*** stands for the solid components (***m***=ore, sinter, fluxing etc).

2.3.2 Heat transfer

The inter-phase heat transfer considers a local effective coefficient which takes into considerations the combined effect of convection and radiation within the packed bed [Akiyama et al, 1992].

$$\dot{E}_g^s = -\dot{E}_s^g = h_{g-s} A_{s-g}\left[T_s - T_g\right] \tag{13}$$

$$h_{s-g} = \frac{k_g}{d_s}\left[2.0 + 0.39\left(Re_{g-s}\right)^{0.5}\left(Pr_g\right)^{1/3}\right] \tag{14}$$

The granular specific surface area is modeled as in eq. 15.

$$A_{s\text{-}g} = \sum_{m}\left(f_m \frac{6\varepsilon_m}{d_m \varphi_m} \right) \tag{15}$$

The variables and symbol with their respective units are summarized in table 2

Table 2 Variables and subscripts used in the mathematical formulation

$A_{s\text{-}g}$	Specific area of the bed [m^2/m^3]		**Subscript**
$\dot{E}_g^s$	Rate of energy exchanged between gas and solid phases (kW)	g	Gas phase
f_m	Volume fraction of solid components (-)	s	Solid phase
F_g^s	Momentum transfer from gas phase to solid phase (N/m^3)	i	Index for chemical reactions
h_{g-s}	Overall heat transfer coefficient between gas and solid (W/m^2 K)	j	Index for phase velocity components
k_g	Thermal conductivity of gas phase (W/mK)	k	Index for phase mass fraction
Pr_g	Prandtl number relating to the gas phase	m	Index to account for phase component

2.3.3 Chemical Reactions

The model takes into consideration major chemical reactions and phase transformations. Additionally, in this work a mechanism of dioxins and furans formation are addressed. Table 3 shows the chemical reactions, phase transformations and dioxins/Furans considered in this model. The rate equations for chemical reactions, phase transformation and PCDDs and PCDFs are found elsewhere (Austin et al, 1997, Castro et al, 2005, 2006)

2.3.4 Dioxins and furans formation

The PCCD/Fs, are groups of chlorinated tricyclic aromatic compounds where different degrees and compounds of chlorination on the aromatic ring structures can occur forming 75 PCDD and 135 PCDF isomers. In the environment PCD/Fs are found in traces quantities as mixture of the isomers and often referred to as “dioxins”. It is believed that Some isomers of dioxin may have carcinogenic and mutagenic effects. Regarding to industrial process, our concern is due to, in high temperature process of sintering iron ore, carbon source materials such as coal and biomasses are used as heat supplier. In the sinter process of iron ore some small amount of dioxins and furans are formed and represent a dangerous contaminant for humans. Although it is well known that PCCD/Fs may be formed in many combustion processes, it is not yet possible completely understand the mechanism of formation, because the chemical reactions are very complex. Involving gas phase, condensed phases. Heterogeneous reactions mechanisms have been proposed in order to explain the formation and destruction of the PCCD/Fs.

In the present work, a kinetic model of PCCD/Fs formation via de novo synthesis is investigated, as presented in table 2. The basic molecule of dioxins and furans are presented in Fig. 4, where are positions occupied by chorine and hydrogen.

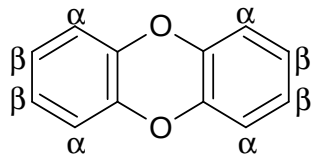

a) Dioxin -PCDDs (Policlorine Dibenzene -p-Dioxin)

$C_{12}O_2H_xCl_{(8-x)}$

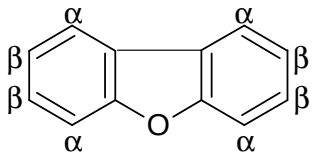

b) Furan-PCDFs (Policlorine Dibenzenefurans)

$C_{12}OH_xCl_{(8-x)}$

Figure 4 Basic structure for dioxin and furan formation

The chemical equations are represented by eq. 24_i, 25_i and 26_i in table 3. Such mechanism was based in "De novo Synthesis" process evaluating the formation of PCDD/Fs in the solid and gaseous phase, according to ashes concentration and partial chlorine pressure. The mechanism rates are represented by eq. 27_i (gas phase) and 28_i (solid phase) in table 3.

2.4 Numerical method

The model equations described above are discretised based on the Finite Volume Method (FVM) where the coupling of velocity and pressure field is done by applying the simple algorithm with staggered covariant velocity components.

The source terms were linearized and the resulting algebraic equations were iteratively solved based on tri-diagonal matrix line by line method (ADI). A computational code based on Fortran 90 was implemented and the computational domain was divided into 20x180x10 control volumes.

Table 3 Chemical reactions considered in the model

R_i	Chemical Reactions
Reduction by CO	
1_i	$\mathbf{3\,Fe_2O_3}(i)+\mathbf{CO}(g)\rightarrow 2\mathbf{Fe_3O_4}(i)+\mathbf{CO_2}(\mathbf{g})$ $(i\rightarrow \text{ore, sin ter, fines, etc})$
2_i	$\frac{\mathbf{w}}{\mathbf{4w-3}}\mathbf{Fe_3O_4}(i)+\mathbf{CO}(g)\rightarrow \frac{3}{4w-3}\mathbf{Fe_wO}(i)+\mathbf{CO_2}(\mathbf{g})$ $(i\rightarrow \text{ore, sin ter, fines, etc})$
3_i	$\mathbf{Fe_wO}(i)+\mathbf{CO}(g)\rightarrow w\,\mathbf{Fe}(i)+\mathbf{CO_2}(\mathbf{g})$ $(i\rightarrow \text{ore, sin ter, fines, etc})$
Reduction by H_2	
4_i	$\mathbf{3\,Fe_2O_3}(i)+\mathbf{H_2}(g)\rightarrow 2\mathbf{Fe_3O_4}(i)+\mathbf{H_2}O(\mathbf{g})$
5_i	$\frac{\mathbf{w}}{\mathbf{4w-3}}\mathbf{Fe_3O_4}(i)+\mathbf{H_2}(g)\rightarrow \frac{3}{4w-3}\mathbf{Fe_wO}(i)+\mathbf{H_2}O(\mathbf{g})$
6_i	$\mathbf{Fe_wO}(i)+\mathbf{H_2}(g)\rightarrow w\,\mathbf{Fe}(i)+\mathbf{H_2}O(\mathbf{g})$ $(i\rightarrow \text{ore, sin ter, fines, etc})$
Re-oxidation of solids	
7_i	$w\,\mathbf{Fe}\ (i)+\frac{1}{2}\mathbf{O_2}(g)\rightarrow \mathbf{Fe_wO}(i)$
8_i	$\frac{3}{4w-3}\mathbf{Fe_wO}(i)+\frac{1}{2}\mathbf{O_2}(g)\rightarrow \frac{\mathbf{w}}{\mathbf{4w-3}}\mathbf{Fe_3O_4}(i)$
9_i	$\mathbf{2\,Fe_3O_4}(i)+\mathbf{O_2}(\mathbf{g})\rightarrow 3\mathbf{Fe_2O_3}(i)$ $(i\rightarrow \text{ore, sin ter, fines, etc})$
Gasification of carbon	
10_i	$C(i)+\frac{1}{2}\mathbf{O_2}(g)\rightarrow CO(g)$
11_i	$C(i)+\mathbf{O_2}(g)\rightarrow CO_2(g)$
12_i	$C(i)+\mathbf{CO_2}(g)\rightarrow 2CO(g)$
13_i	$C(i)+\mathbf{H_2}O(g)\rightarrow H_2(g)+CO(g)$ $(i\rightarrow \text{coke breeze or coal})$
Gasification of volatiles	
14_i	$\text{Volatiles}(i)+\alpha_1O_2(g)\rightarrow \alpha_2CO_2(g)+\alpha_3H_2O(g)+\alpha_4N_2(g)$
15_i	$\text{Volatiles}(i)+\alpha_5CO_2(g)\rightarrow \alpha_6CO(g)+\alpha_7H_2(g)+\alpha_8N_2(g)$ $(i\rightarrow \text{coke breeze or coal})$
Water gas shift	
16	$CO_2(g)+H_2(g)\rightarrow CO(g)+H_2O(g)$
Phase transformation	
17_i	$H_2O(i)\leftrightarrow H_2O(g)$ $(i\rightarrow \text{ore, sin ter, coke})$
18_i	$CaO(i)\leftrightarrow CaO(l)$
19_i	$MgO(i)\leftrightarrow MgO(l)$
20_i	$MnO(i)\leftrightarrow MnO(l)$
21_i	$Al_2O_3(i)\leftrightarrow Al_2O_3(l)$ $(i\rightarrow \text{ore, sin ter, coke})$
22_i	$CaO(i)+FeO(i)\leftrightarrow (CaO).(FeO)$ $(i\rightarrow \text{ore, sin ter, coke})$
23_i	$2CaO(i)+FeO(i)\leftrightarrow (CaO)_2.(FeO)$ $(i\rightarrow \text{ore, sin ter, coke})$
Dioxin formation and rate formation	
24_i	$48\,C_{(s)}+2.5\,O_2+16\,HCl_{(g)}+4\,H_{2(g)}\leftrightarrow C_{12}OH_5Cl_{3(g)}+C_{12}O_2H_5Cl_{3(g)}+$ $+\,2\,C_6H_3Cl_2OH_{(g)}+2\,C_6H_3Cl_{3(g)}$
25_i	$2\,\left[C_6H_3Cl_2OH_{(s)}\right]\rightarrow C_{12}OH_5Cl_{3(s)}+HCl_{(g)}+H_2O_{(g)}$
26_i	$C_6H_3Cl_2OH_{(s)}+C_6H_3Cl_{3(s)}+0.5O_{2(g)}\rightarrow C_{12}O_2H_5Cl_{3(s)}+2HCl_{(g)}$
27_i	$\frac{dm_{PCDD/Fs}}{dt}=\frac{0.38\times10^9 C_{Ash}}{\rho d}\left[0.72\frac{\alpha P}{\sqrt{T}}-3.7\times10^{13}\exp\left(-\frac{2.0\times10^4}{T}\right)X_P\right]$
28_i	$\frac{dm_{PCDD/Fs}}{dt}=3.0\times10^{-1}\exp\left(-\frac{10,500}{T}\right)[Cl_{Ph}][Cl_{Bz}]$

3. RESULTS AND DISCUSIONS

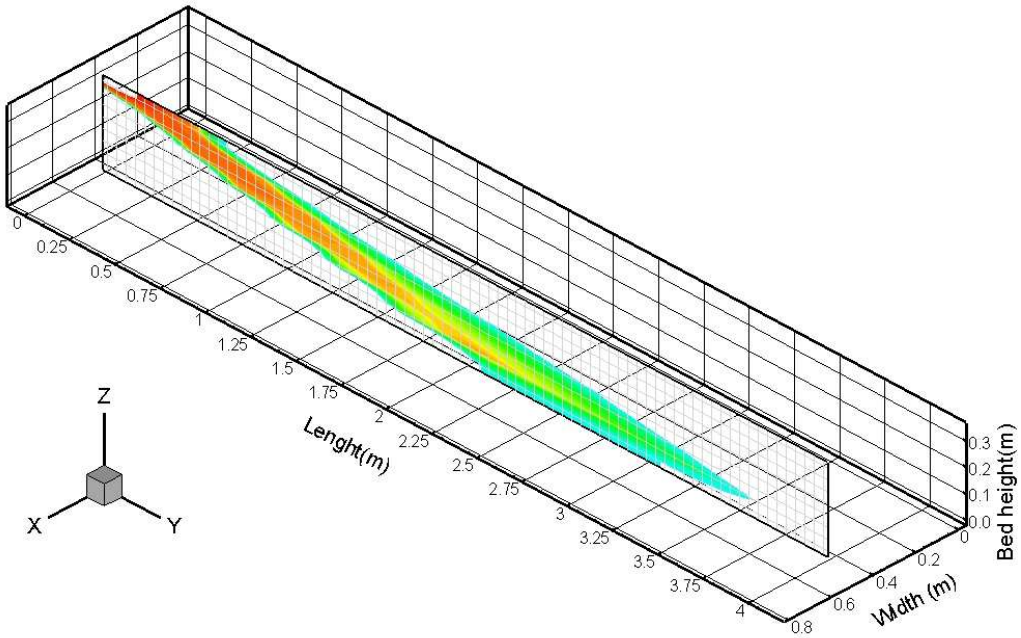

Figure 5 Thermal and chemical propagation front for a conventional sintering operation

Figure 5 shows the combustion front within the sinter bed where is observed high temperature and partial melting of raw materials. The region above the sinter front is the cooling zone where re-oxidation and solidification of sinter cake takes place. The shape and the thickness of the combustion front plays important role on the final sinter properties, therefore the model predictions is an important tool to help operators set up the conditions of strand velocity gas flow rates and so on. In order to validate the model predictions temperature measurements were carried out by inserting thermocouples into the interior of the sinter bed and operational conditions set up were registered. Then, the model was run and compared. Model predictions of temperature and thermocouples results are shown in Fig. 6a and b. In Figure 6a, the thermocouples were placed 5 cm depth of the sinter layer while for Figure 6b the thermocouples were located at the inlet of wind boxes. Both comparisons have shown good agreement which validated the model approach.

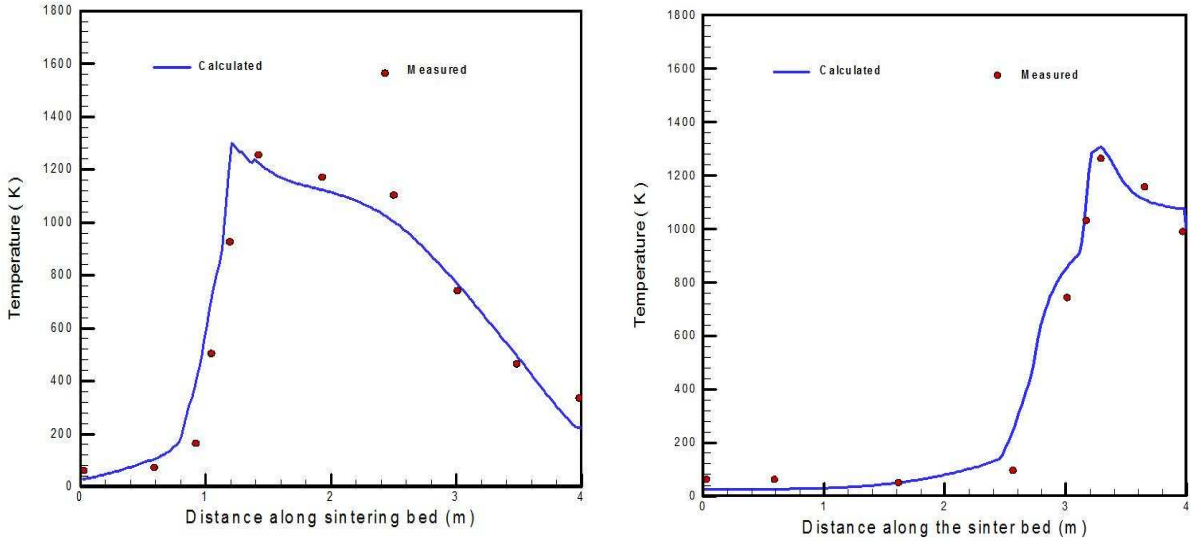

a) Temperature 5 cm from surface

b) Temperature at outlet boxes

Figure 6 Comparison of temperature measurements and model predictions for industrial scale operation

The next step was to investigate the dioxins and furans behavior in the interior of sinter bed. Following the model formulation the dioxins, furans and precursors where calculated for both gas and solid phases. Figure 7 depicts dioxins, chlorobenzene and phenol concentration in the gas phase while Figure 8 shows dioxins and furans absorbed in the solid phase.

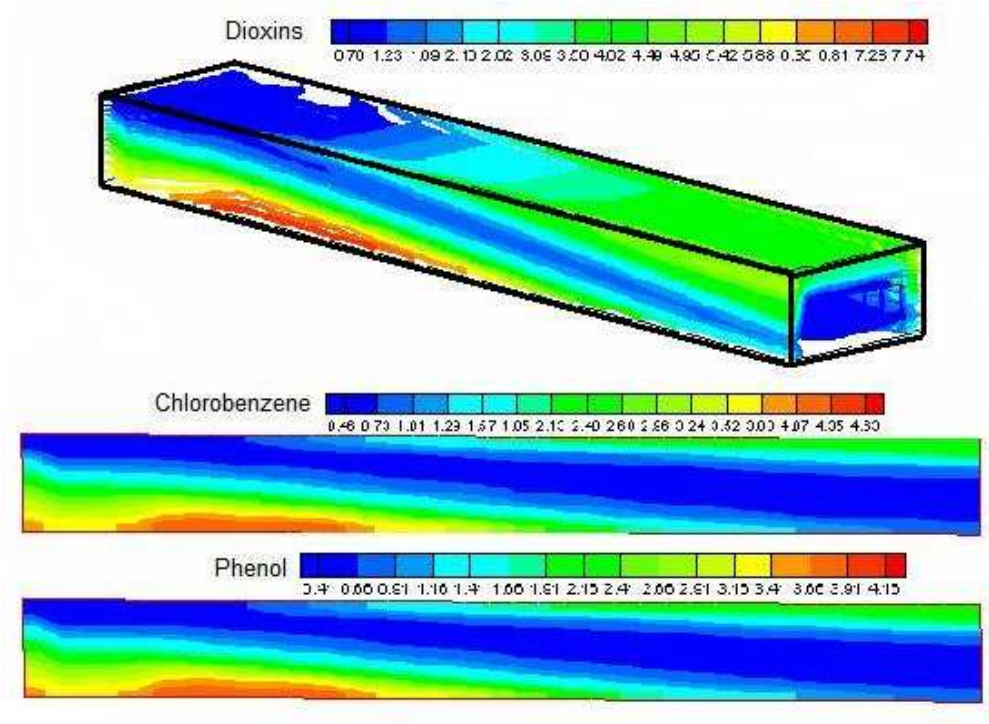

Figure 7 Dioxins and precursor predictions for gas phase

Experimental investigation has pointed out that the dioxins and furans are formed in a temperature range of 250 - 450ºC under cooling conditions. Such thermodynamics conditions is encountered in the region just below the combustion zone in the intermediated wind boxes due to enough residence time. The same conditions are present at the ending boxes, however the residence time was not sufficient to form significant amount of dioxins and furans. Regarding to the solid phase the opposite situation is observed and the higher amount of dioxins are obtained at the outlet within the lower layers. Another important parameter is the composition of iron ore raw materials which can contains Cu, an strong PCDD/Fs catalyst increasing considerably the final amount of substances formed. In this investigation, the effect of Cu catalyst was not investigated due to the kinetics mechanism was not incorporated into the model. Previous experimental work, however, suggested that the raw materials for iron ore sintering should have less than 2 ppm of Cu content to avoid the catalyst strong effect, (Harjanto et al, 2002).

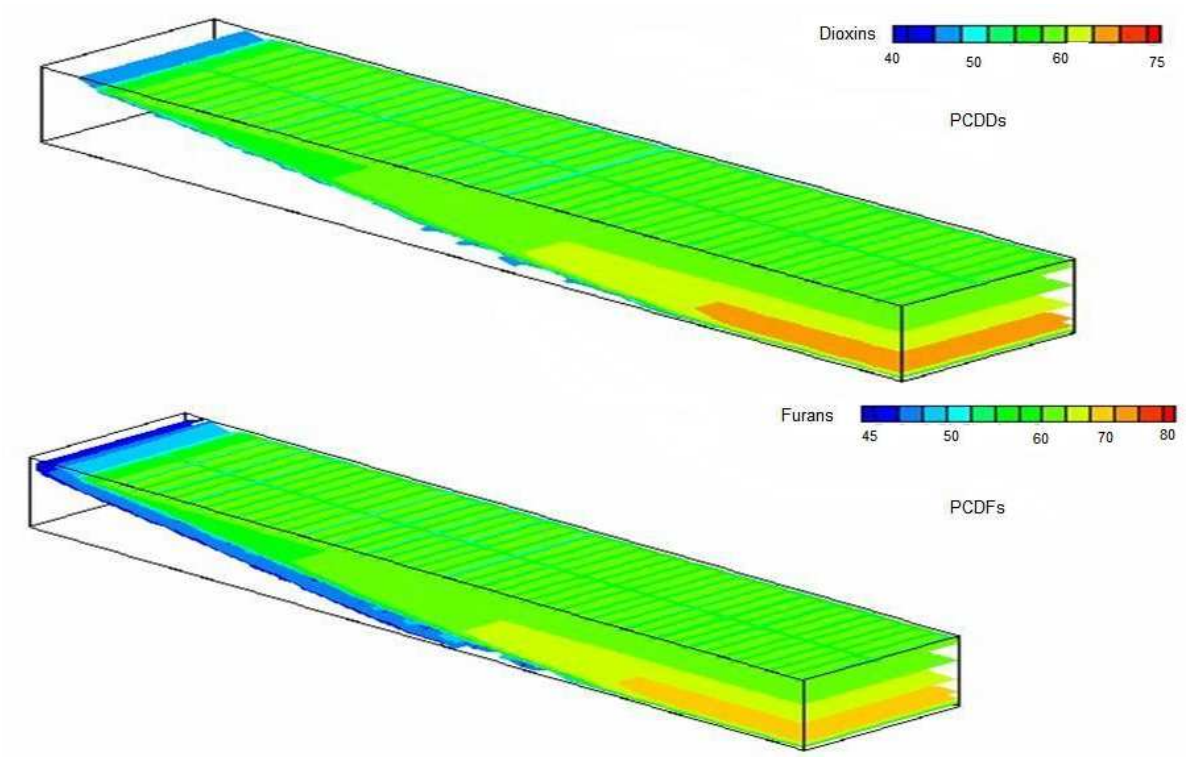

Figure 8 Model predictions of dioxins and furans in the solid phase of the iron ore sinter strand process

4. CONCLUSIONS

A multiphase multi-component mathematical model for the iron ore sinter process has been developed and applied to investigate the emissions of PCDD/Fs of the sinter plant of an integrated steel industry. The model is based on transport equations of momentum energy and chemical species coupled with chemical reaction of reduction, combustion, oxidation and physical transformation such as melting, water evaporation and condensation and PCDD/Fs absorption and formation. The computational code was implemented in Fortran 90/95 and the finite volume method based on the SIMPLE algorithm with staggered co-variant velocity projections. The model results were confronted with industrial measurements of temperature by thermocouples located within the sinter bed and showed good agreement. The model was used to investigate optimum operational conditions which minimize the formation of PCDD/Fs. Simulation results indicated that with recirculating gas and increasing the permeability of the sinter bed the residence time of gas into the favorable zone decreases and reduce the emissions into the flue gas to around 20 ng/Nm^3. On another hand, the strand velocity can be increased and the adsorption into the solid phase could be decreased, however a strict control of the operational conditions is necessary, since these actions usually increase the amount of return sinter and hence, decreases the productivity. In spite of these troublesome, simulations results indicated that a sinter product with PCDD/Fs less than 50 ng/t is obtained.

5. ACKNOWLEDGEMENTS

The authors thanks to CAPES and CNPq (Research grant – PQ2006) for the financial support on the development of this project

6. REFERENCES

Akiyama, T. Ohta, H. Takahashi, R. Waseda, O. and Yagi, J. , 1992 “Measurement of Oxide and Porous Modeling of lron Ore Thermal Conductivity for Dense iron Agglomerates in Stepwise Reduction”, ISIJ International., Vol. 32, pp. 829-837.

Austin, P.R., Nogami, H. and Yagi, J., 1997, “A Mathematical Model of Four Phase Motion and Heat Transfer in the Blast Furnace”, ISIJ International., Vol. 37, pp. 458-467.

Austin, P.R., Nogami, H. and Yagi, J., 1997, “A Mathematical Model for Blast Furnace Reaction Analysis Based on the Four Fluid Model”, ISIJ International, Vol. 37, pp. 748-755.

Castro, J.A., Nogami, H. and Yagi, J., 2006, “Industrial Process Simulation Based on Multiphase Mathematical Model: Application to Predict the Sinter Plant Operation” Proceedings of the 11th Brazilian Congress of Thermal Sciences and Engineering -- ENCIT 2006, Curitiba, Brazil, pp. 1-10

Castro, J.A. Silva, A.J. , Nogami, H. e Yagi, J. , 2005, “ Tecnologia em Metalurgia e Materiais, Vol 2, pp 45-52.

Castro, J.A., Nogami, H. and Yagi, J., 2002, “Three-dimensional Multiphase Mathematical Modeling of the Blast Furnace Based on the Multifluid Model”, ISIJ International., Vol. 42, pp. 44-52.

Castro, J.A, 2001, “A multi-dimensional transient mathematical model of the blast furnace based on the multi-fluid model”. Ph.D thesis, IMRAM – Institute for multidisciplinary research for advanced materials – Tohoku University – Japan

Cumming, M.J. and Thurlby, J. A., 1990 “Development in Modelling and Simulation of Iron Ore Sintering”, Ironmaking and Steelmaking, vol 17, pp 245-254.

Harjanto, S., Kasai,E., Terui, T. and Nakamura, T. “Behavior of Dioxin During Thermal Remediation in the Zone Combustion Process, 2002, Chemosphere, vol. 47, pp.687-693.

Kasai, E. Batcaihan, B. Omori, Y. Sakamota, N. and Kumasaka, A., 1991 “Permeation Characteristics and Void Structure of lron Ore Sinter Cake”, ISIJ International., Vol. 31, pp. 1286-1291.

Mitterlehner, J. Loeffler, G. Winter, F., Hofbauer, H., Schmid, H. Zwittag, E. , Buergler, H. Pammer, O. and Stiansy, H., 2004 “Modeling and Simulation of Heat Front Propagation in the Iron Ore Sintering Process”, ISIJ International., Vol. 44, pp. 11-20.

Nath, N. K. Silva, A.J. and Chakraborti, N. , 1997 “Dynamic Process Modelling of Iron Ore Sintering”, Steel Research, vol 68, pp 285-292.

Waters, A. G. Litster, J.D. and Nicol, S.K., 1989 “AMathematical Model for the Multicomponent Sinter Feed”, ISIJ International, Vol. 29, pp. 274-283.

7. RESPONSIBILITY NOTICE

The authors are the only responsible for the printed material included in this paper.